Available online at www.sciencedirect.com
ScienceDirect
Icarus 190 (2007) 224–235
ICARUS
www.elsevier.com/locate/icarus

# The origin and distribution of the Centaur population

Romina P. Di Sisto *, Adrián Brunini

*Facultad de Ciencias Astronómicas y Geofísicas (UNLP) and Instituto de Astrofísica de La Plata (CONICET) Paseo del Bosque s/n (1900) La Plata, Argentina*

Received 7 September 2005; revised 19 February 2007

Available online 13 March 2007

**Abstract**

We analyze the Centaur population as a group of objects with perihelion distances ($q$) of less than 30 AU and heliocentric distances outside the orbit of Jupiter, formed by objects entering this region from the Scattered Disk (SD). We perform a numerical integration of 95 real Scattered Disk Objects (SDOs) extracted from the Minor Planet Center database and of 905 synthetic SDOs compensating for observational biases. SDOs have in the Centaur zone a mean lifetime of 72 Myr, though this number falls with a decrease of $q$. After this incursion, 30% of them enter the zone interior to Jupiter's orbit. We find that the contribution to the Centaur population from the SD gives a total of $\sim 2.8 \times 10^8$ Centaurs with a radius $R > 1$ km. We also propose a model for the intrinsic distribution of orbital elements of Centaurs and their distance and apparent magnitude distribution.


*Keywords:* Centaurs; Trans-neptunian objects

## 1. Introduction

Centaurs have a transitory nature being an intermediate state as bodies from the Trans-Neptunian Region (TNR) or the Edgeworth–Kuiper Belt (EKB) in transit to the Jupiter Family Comet (JFC) zone. There is not a universally accepted definition of Centaurs. They can be defined by a semimajor axis $a$ between 5 and 30 AU, by a perihelion distance $q$ in this same range or according to the Tisserand parameter ($T$) with respect to Jupiter being $T > 3$ and $a > a_J$ where $a_J$ is the semimajor axis of Jupiter. Nevertheless, it is generally accepted that they are objects which enter the planetary region from the TNR evolving towards the JFC zone (Fernández, 1980; Duncan et al., 1988; Levison and Duncan, 1997).

At present, it is possible to identify three characteristic kinds of dynamical groups in the TNR (Chiang et al., 2006): the classical objects (CKBO), with $a$ greater than ∼42 AU, low eccentricity and non-resonant orbits; the resonant objects, those in mean motion resonance with Neptune (the 3:2 resonance, where there are plutinos, is the most populous one); and the Scattered Disk Objects (SDOs) with $q > 30$ AU and $a > 50$ AU in large eccentricity orbits. Levison and Duncan (1997) studied the evolution of 20 TNO with $\sim 34 < a < \sim 44$, eccentricities $e < 0.05$ and inclinations $i < 16°$ plus clones. They found, as a sub-product of this evolution, a group of objects in Neptune crossing orbits and scattered by this planet, which they called Scattered Disk Objects. They also proposed that there must be a large population of objects in the SD. Duncan and Levison (1997) gave another explanation for the SD as objects scattered by Neptune during the evolution of the Solar System—a version that is currently more accepted (Morbidelli et al., 2003).

SDOs are capable, through encounters with Neptune, of evolving into the planetary region, becoming Centaurs.

The goal of this work is to study the Centaur population through numerical simulations, taking into account the contribution of the SD. We accept as a definition of Centaurs those objects with $q < 30$ what distinguish them from SDOs (Tiscareno and Malhotra, 2003).

Tiscareno and Malhotra (2003) numerically investigate the dynamical behavior of observed Centaurs for $10^8$ years under the perturbations of the four giant planets. They present a general model of the Centaur population obtained through their integration.

Horner et al. (2004a, 2004b) dynamically integrate 23,328 particles based on the orbits of 32 well-known Centaurs for

* Corresponding author.
*E-mail address:* romina@fcaglp.unlp.edu.ar (R.P. Di Sisto).

0019-1035/$ – see front matter 
doi:10.1016/j.icarus.2007.02.012

3 Myr. In the first paper they broach the Centaur population as a whole and in the second one they focus on individual objects.

Emel'yanenko et al. (2005) carried out a numerical study of orbits based on observed objects with perihelion distances $q$ in the range $28 < q < 35.5$ AU and semimajor axes $a$ in the range $60 < a < 1000$ AU to predict the orbital distribution of Centaurs in the zone $5 < q < 28$ AU. They argued that most Centaurs come from the Oort cloud. But, on the one hand they only integrated SDOs with $60 < a < 1000$ AU. Fernández et al. (2004) have shown that the resonances in the region $50 < a < 60$ AU are important residence niches of SDOs, and in fact, the dynamical evolution in this region cannot be considered a random walk in energy. Therefore, any study of the link between SDOs and Centaurs should consider these resonances. Besides, in the region $60 < a < 170$ AU, there are several mean motion resonances at high eccentricities that are even stronger than the ones at $a < 60$ AU, making the distinction between these two initial populations rather artificial. High eccentricity initial conditions as the ones used by Emel'yanenko et al. (2005) correspond to orbits less bounded, and therefore more affected by the "Neptune's dynamical barrier" (as discussed in Fernández et al., 2004), and are more prone to diffuse outwards before becoming a Centaur by the action of planetary or, more likely, external perturbations. On the other hand, Emel'yanenko et al. (2005) initial conditions are partially corrected by the observational bias in inclination, as discussed in Brown (2001).

The achievement of our work is to investigate the Centaur population studying their evolution from objects in their main source and following them for the age of the Solar System. This is a long-term integration in contrast with the papers by Horner et al. (2004a, 2004b), and we begin our study in the Centaur source, in contrast with Tiscareno and Malhotra (2003)'s paper. In the following sections, we will compare some of their results with ours.

Descriptions of the initial conditions and of the simulation are given in the next section. In Section 3, we present the general outcomes of the simulation. In Section 4, we estimate the number of Centaurs. In Section 5, we describe the general dynamical evolution in the Centaur zone. In Section 6, we present the intrinsic distribution of orbital elements, distance and magnitudes of Centaurs. Section 7 is devoted to conclusions.

## 2. Numerical simulation

### 2.1. Scattered Disk Objects

Scattered Disk Objects are then defined by their perihelion distance $q > 30$, but they are also limited in their semimajor axes to those with $a > 50$ AU. In the Minor Planet Center database,[1] SDOs as previously defined, appear together with Centaurs. Whatever the origin of the SD was, SDOs have perihelion distances under the control of Neptune, so there should also be SDOs with semimajor axes of less than 50 AU. However, the zone of objects with $a < 50$ AU is plenty of CKBOs and it is difficult to discern one from another. So, in order not to mix those populations but to have a complete sample of the SD, we selected from the Minor Planet Center database of TNOs[2] as SDOs in the zone of $40 \text{ AU} < a < 50$ AU, those objects with $30 \text{ AU} < q < 39$ AU and eccentricities $e > 0.2$. This limit in eccentricity is also considered as a distinguishing feature between CKBOs and SDOs in Elliot et al. (2005). We chose these objects together with the SDOs with $a > 50$ AU and $30 \text{ AU} < q < 39$ AU from the MPC databases in November 2004. They are 32 objects in the zone $40 \text{ AU} < a < 50$ AU and 63 with $a > 50$ AU. From the list of SDOs and Centaurs, we removed those objects with $q > 39$ AU that probably belong to the Extended Scattered Disk (ESD) (Gladman et al., 2002), a region that would be part of a primordial trans-neptunian belt not tied to the Neptune scattering process. In Fig. 1, we show SDOs as we have previously defined them, plutinos, CKBOs and ESDOs. Fig. 2a shows the distribution of the real SDOs of our sample in semimajor axis.

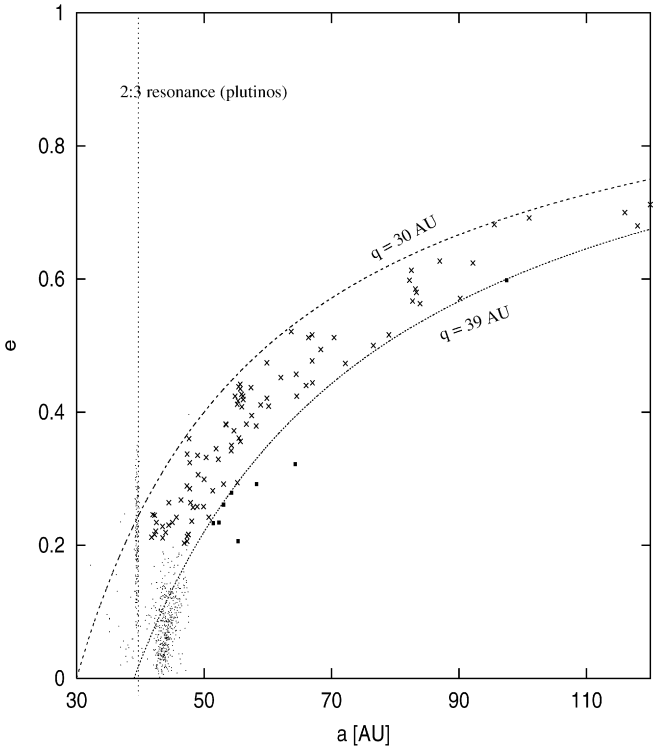


Fig. 1. Observed SDOs as defined in Section 2 (crosses), classical TNOs and plutinos (dots), ESDO (filled squares). The curves of perihelion distances $q = 30$ AU and $q = 39$ AU, that limit our initial orbits (for eccentricities greater than 0.2) are also shown.

### 2.2. The integration and initial conditions

We performed a numerical integration of 95 real SDOs extracted from the Minor Planet Center database as explained before, and of 905 synthetic SDOs, for a total of 1000 particles. We considered the real and the synthetic SDOs to be massless particles under the gravitational influence of the Sun (including

[1] http://cfa-www.harvard.edu/iau/lists/Centaurs.html.

[2] http://cfa-www.harvard.edu/iau/lists/TNOs.html.

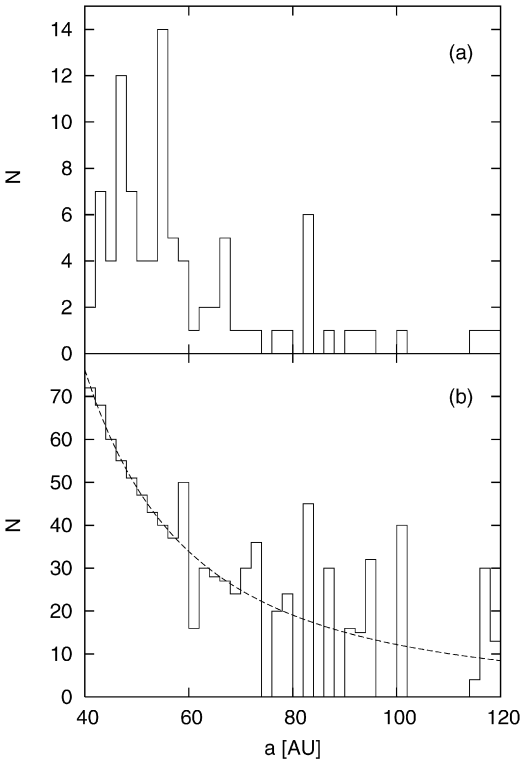


Fig. 2. (a) Semimajor axis distribution of the real SDOs of our sample. For clarity, the two real objects with $a > 200 AU$ of our sample were omitted in this figure. (b) Semimajor axis distribution of all the SDOs (real + synthetic SDOs) of our initial conditions. The dotted line represent the power law distribution of SDO's semimajor axis given by Eq. (3).

the masses of the terrestrial planets) and the four giant planets. The simulation was performed with the hybrid integrator EVORB (Fernández et al., 2002) with an integration step of 0.5 years. Each particle evolved for 4.5 Gyr, unless removed due to a collision with a planet, to reaching a semimajor axis $a > 1000$ AU, or to entering the region inside Jupiter's orbit ($r < 5.2$ AU), where the perturbations of the terrestrial planets are not negligible.

### 2.2.1. Initial semimajor axis distribution

The number of synthetic SDOs were generated in the same way as they were in Fernández et al. (2004), i.e. to account for the bias in the discovery probability for different semimajor axes.

If we assume that SDOs can be discovered when they are close to their perihelia (say within a limiting heliocentric distance $r_L$), then from Kepler's equation, the fraction of time that the body remains within the reach of Earth's observers (i.e. with $r < r_L$) is

$$\tau = \frac{\Delta T}{P} = \frac{1}{\pi}\big(\varepsilon_L - e\sin(\varepsilon_L)\big), \tag{1}$$

where $\Delta T$ is the time that the body has $r < r_L$, $P$ is its orbital period and $\varepsilon_L$ is the eccentric anomaly corresponding to $r_L$ given by

$$\varepsilon_L = \cos^{-1}\left(\frac{1}{e}(1 - r_L/a)\right). \tag{2}$$

Applying the correction fraction given by Eq. (1), we found that the distribution of semimajor axes of SDOs follows approximately the power-law

$$f(a)\,\mathrm{d}a \propto a^{-\beta}\,\mathrm{d}a, \tag{3}$$

where $\beta = 2$. We have divided the real sample in bins of 2 AU. Next, we have generated a series of random numbers, each one representing a semimajor axis, in the region of $a$ occupied by the real SDOs and following the distribution given by Eq. (3). If the semimajor axis generated by this procedure lie inside an empty bin of the real sample, this semimajor axis was discarded. In this way, we have obtained a distribution of 1000 random semimajor axes with the desired distribution. This distribution is shown in Fig. 2b. The number of synthetic SDOs we have to generate for each one of the bins in $a$ is simply the difference between the histograms shown in Figs. 2a and 2b. All these synthetic SDOs were created from the real SDOs by generating their initial mean anomaly at random in the interval $[0°, 360°]$ with uniform distribution.

As for some real SDOS we have to generate a very large number of synthetic SDOs, we also change the semimajor axis by an amount $\delta$, for nearly half (taken at random from the total sample of synthetic SDOs) of them in order to guarantee that synthetic SDOs are really different one of each other. $\delta$ being a small random number in the interval $(-2 \times 10^{-4}, 2 \times 10^{-4})$ it does not change the overall distribution of $a$ previously obtained. This strategy also takes into account the decrease in the accuracy of the orbit determination with $a$.

Up to now, we have 1000 SDOs with 40 AU $< a <$ 227 AU that follow the unbiased distribution of semimajor axes of SDOs used by Fernández et al. (2004).

### 2.2.2. Initial inclination distribution

There is also an observational bias that affects the inclinations of observed SDOs. The observed distribution of KBO inclinations includes inclinations as high as 40°. But, the observational surveys are strongly biased towards low inclinations. Brown (2001) estimates the inclination distribution for the three classes of KBOs by linking the real distribution of KBO inclinations to the inclination distribution of bodies crossing the ecliptic at any time. For SDOs in particular he obtained

$$F(i)\,\mathrm{d}i \propto \sin i \exp^{-i^2/2\sigma_i^2}, \tag{4}$$

where $\sigma_i = 20°$.

However, this method is based on considering circular orbits for the KBOs, which is far from reality. SDOs have large eccentricities, so this law is only an approximation. A better fit to the parameters of the law obtained by Brown (2001) is given in Morbidelli et al. (2003) who propose a value $\sigma_i = 12°$ based on a model in which the high inclinations observed in the KB (the three populations) had a common origin as primordial scattered objects originally coming from an inner denser region of the original planetesimal disk (Gomes, 2002). This new $\sigma_i$ value for SDOs is near the value for CKBOs and Plutinos.

We also changed the inclinations of all the synthetic SDOs in order to fit the total distribution of inclinations to that given by Eq. (4), with $\sigma_i = 12°$.

We proceeded as follows: we took bins of 1° from inclinations between 0° and 40° noticing how many particles we should have in each bin according to Eq. (4). We subtracted from this number the number of real SDOs that are in each bin, obtaining then the number $N_i$ of synthetic SDOs to which we had to change the inclinations. We took at random from our synthetic SDOs sample $N_i$ particles giving them an inclination at random between the minimum and maximum value of the inclination in this bin. The process follows until all the synthetic SDOs have random inclinations, and the total sample is finally distributed according to Eq. (4). The distribution of inclinations of our initial conditions are shown in Fig. 3 where the theoretical distribution given by Eq. (4) is also shown.

## 3. General results

The results of our integration are first classified according to zones of particle's initial conditions. Because of the nature of SDOs we divided them first according to their perihelion distance being less or more than 35 AU, and then in intervals of semimajor axes. In Table 1 we show, for each initial zone, the number of particles and the percentages of particles that: collide with a planet, reach the zone of $r < 5.2$ AU, survive the total integration time, are ejected from the Solar System and the ratio between number of ejected and survivor particles. We also show the percentage of particles from each zone that are Centaurs for some time, and the corresponding mean lifetimes in this state. We have 4 collisions with Neptune and 1 with Saturn. 25.8% of the particles survive the total integration time, 51.9% are ejected from the Solar System, and 21.8% enter the zone interior to Jupiter's orbit. There is a strong dependence on $q$ of the relation: number of ejected ($N_e$)–number of survivors ($N_s$) particles. The ratio $N_e/N_s$ is always greater than 1 for $q < 35$ AU, though for $a < 50$ it is greater than for $a > 50$ AU, where it does not change so much. For the zone $q > 35$ AU and $40 < a < 50$, $N_e/N_s$ is only a bit greater than 1 (in contrast with the zone of $q < 35$ AU), but for $q > 35$ AU and $a > 50$ $N_e/N_s$ is less than 1. This is consistent with the fact that the perturbation of Neptune in this zone is weak, so it is more stable. But, $N_e$ is incomplete because particles are not followed when they reach the zone of $r < 5.2$ AU. Nevertheless we can speculate that it is probable that almost all these particles will be finally ejected and then they should be gather to $N_e$. If this were the case, the behavior of the relation $N_e/N_s$ with the initial perihelion zone and semimajor axis zone will be the same, and may be calculated from the numbers in Table 1.

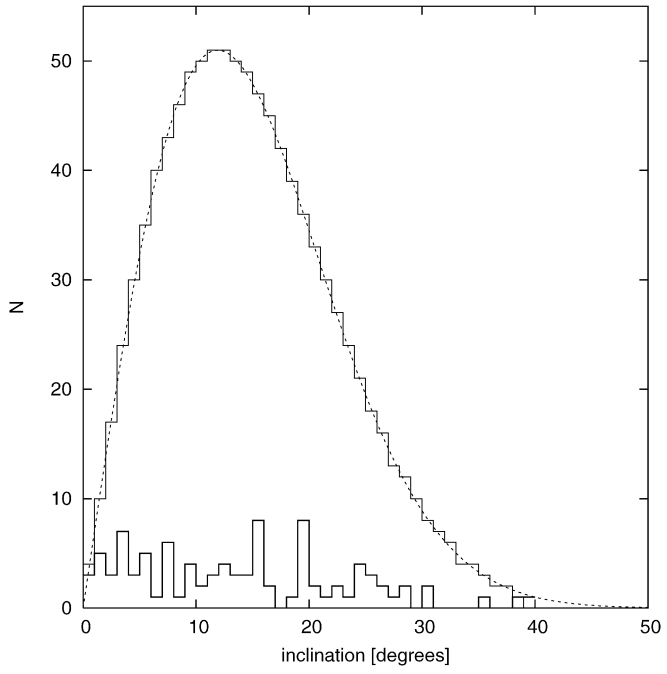


Fig. 3. Histograms showing the distribution of inclination of our initial conditions and of the real SDOs. The dashed curve is the theoretical distribution given by Eq. (4) (see main text).

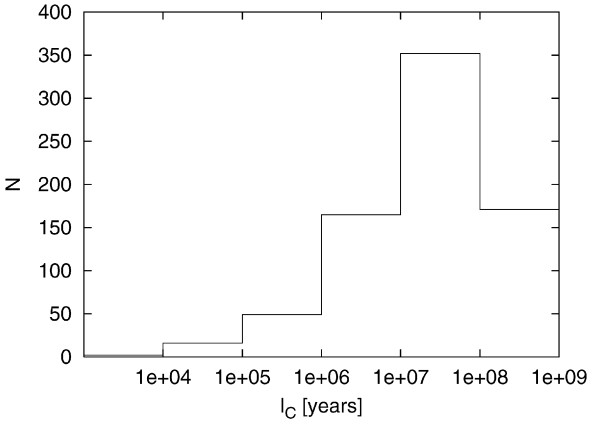


Fig. 4. Number of particles against lifetime in the Centaur zone for all SDOs in our simulation.

Table 1
Number of particles ($N_p$) in each initial zone according to initial perihelion distance ($q$) and semimajor axis ($a$)

| $N_p$ | | | Col. | $r < 5.2$ AU | Surv. | Eject. | $N_e/N_s$ | $q < 30$ | $l_C$ [$10^6$ y] |
|---|---|---|---|---|---|---|---|---|---|
| 246 | $q < 35$ | $40 < a < 50$ | 0.8 | 37.8 | 6.5 | 54.9 | 8.5 | 96 | 81 |
| 146 | $q < 35$ | $50 < a < 60$ | 0.7 | 26.7 | 11 | 61.6 | 5.6 | 90 | 61 |
| 68 | $q < 35$ | $60 < a < 70$ | 1.5 | 20.6 | 13.2 | 64.7 | 4.9 | 88 | 108 |
| 89 | $q < 35$ | $70 < a < 90$ | 0 | 14.6 | 12.4 | 73 | 5.9 | 89 | 55 |
| 130 | $q < 35$ | $a > 90$ | 0 | 10 | 13 | 77 | 5.9 | 89 | 82 |
| 60 | $q > 35$ | $40 < a < 50$ | 0 | 23.3 | 33.4 | 43.3 | 1.3 | 67 | 73 |
| 261 | $q > 35$ | $a > 50$ | 0.4 | 12.2 | 64.8 | 22.6 | 0.4 | 36 | 46 |

Percentages of particles that: collide with a planet, reach the zone of $r < 5.2$ AU, survive the total integration time, are ejected from the Solar System and the ratio between number of ejected and number of survivor particles. The last two columns show the percentage of particles that are Centaurs ($q < 30$), and the corresponding mean lifetimes in this state.

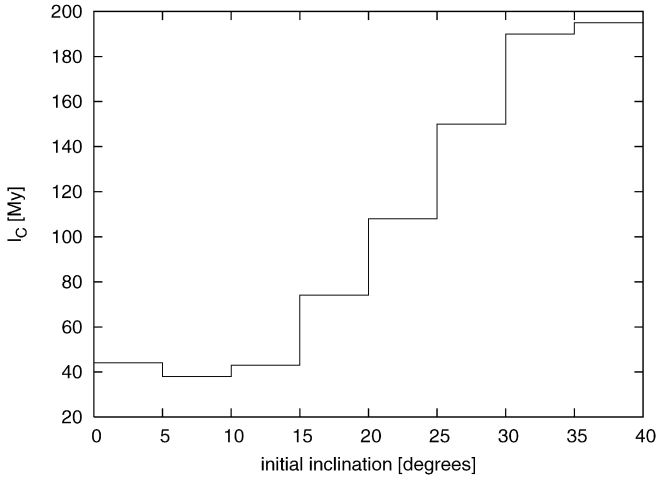


Fig. 5. Mean lifetime of SDOs in the Centaur zone versus initial inclinations.

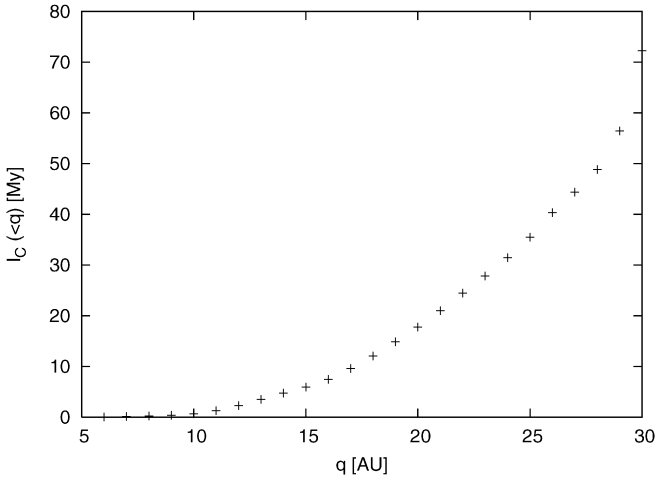


Fig. 6. Mean lifetime of SDOs in the Centaur zone with perihelion distance $q$ less than a given value.

There is an evident correlation with the initial perihelion distance and also with the initial semimajor axis of particles that reach the zone of $r < 5.2$ AU. We have the greatest contribution (∼40% of the particles in the zone) from objects with $q < 35$ AU and $40 < a < 50$ AU.

In all, 75.5% of our initial particles enter the Centaur zone and the mean lifetime ($l_C$) is 72 Myr. This number is calculated as the sum of each particle's time spent in the Centaur zone divided by the total number of particles that go through the Centaur zone. In Fig. 4 we plot the distribution of lifetimes in the Centaur zone for all SDOs of our simulation. Most of the particles have lifetimes between 10 and 100 Myr. In Fig. 5 we plot the mean lifetime of Centaurs for different initial inclinations $i_i$. We find that higher inclinations produce longer-lived Centaurs. For $i_i < 16°$, which is the limit in Levison and Duncan (1997) integration, we have a mean lifetime of 42 Myr with a standard error of the mean of 1 Myr. Levison and Duncan (1997) obtained a mean lifetime for ecliptic comets (those objects with Tisserand parameter $T > 2$, a group that includes JFCs as well as Centaurs), of 45 Myr.

Moreover, we evaluated the mean lifetime as a function of the perihelion distance ($q$) and we plotted it in Fig. 6. There is a strong dependence of Centaurs lifetime on their perihelion distance. Tiscareno and Malhotra (2003) obtained a mean lifetime of 9 Myr. However they used the observed Centaur population that is strongly biased to low perihelion distances. 70% of observed Centaurs have $q < 17$ AU. In Fig. 6 we have mean lifetimes of less than 10 Myr for objects with $q < 17$ AU. We also calculated the lifetime of particles in the zone of $5.2 < a < 30$, and we obtained 7.6 Myr, a number that is similar to those usually obtained when Centaurs are defined in terms of $a$. Also, we can compared our results with the ones obtained by Horner et al. (2004a, 2004b) (despite their shorter integration) limiting our Centaurs to those with aphelion distances less than 40 AU and $a < 29$ AU (as their sample of Centaurs are). We obtained a mean lifetime of 6.2 Myr and Horner et al. (2004a, 2004b) obtained a mean lifetime of 2.7 Myr.

We considered an encounter with a planet if the particle had a close approach at a distance of less than 3 Hill radii. This limit for a close encounter is related to numerical aspects of our code (see Fernández et al., 2002, for a report on this code). This numbers can be related to the number of encounters within the Hill's sphere simply by dividing them by $3^2$.

We have a total of 1,301,937 encounters with 666 particles. All these particles encounter Neptune. The encounters with Neptune represent 78.22% of the total number of encounters; 488 particles encounter Uranus, representing 18.32% of the encounters; 380 particles encounter Saturn, representing 3.4% of the encounters, and 142 particles encounter Jupiter, representing 0.06%. However, the number of encounters with Jupiter, in particular, is conditional on the removing of objects in the simulation at a distance of Jupiter.

## 4. The number of Centaurs

To estimate the injection rate of Centaurs from the SD, we track, every 10,000 years, the number of SDOs that have reached $q < 30$ AU. These Centaurs can get out of the Centaur region in a future time (and eventually get in again), but, because we want to know the rate of injection of objects from the SD, we need to know when a SDO enters the Centaur zone for the first time. And we consider this object as a Centaur at that time. We plot in Fig. 7 the number of SDOs that have reached the Centaur zone ($N_C$) with respect to the number of SDOs that have remained in the SD ($N_{\rm SDO}$) as a function of time. This ratio is well fitted by the linear relation:

$$\mathrm{d}[N_C/N_{\rm SDO}]/\mathrm{d}t = Y \tag{5}$$

where $Y = 5.2 \times 10^{-10} N_{\rm SDO}$/year is the rate of injection of Centaurs from the SD.

So, in order to estimate the present number of Centaurs ($N_{\rm PC}$) coming from the SD,

$$N_{\rm PC} = Y N_{\rm SDO} l_C, \tag{6}$$

where now $N_{\rm SDO}$ is the total population of the SD. Taking $N_{\rm SDO}$ ($R > 1$ km) $= 7.5 \times 10^9$ from Fernández et al. (2004) as the present number of SDOs (assuming that $N_{\rm SDO}$ is constant with $t$) and $l_C = 72$ Myr from our simulation, we have a

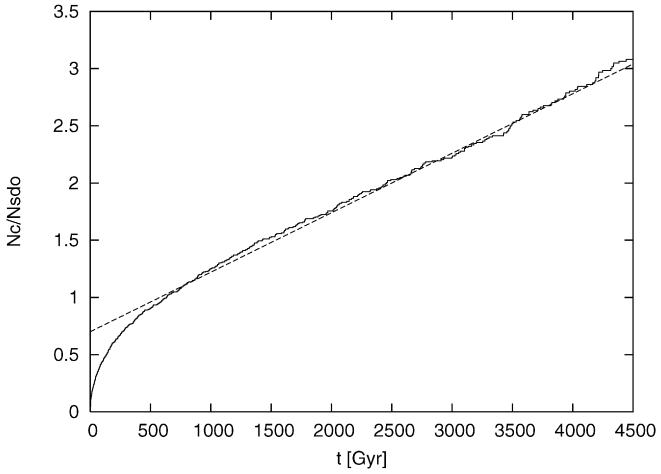


Fig. 7. Number of injected Centaurs $N_C$ from the SD in relation to the number of remaining SDOs ($N_{SDO}$) against time (solid line). The dash line is the fitting to the data (see text).

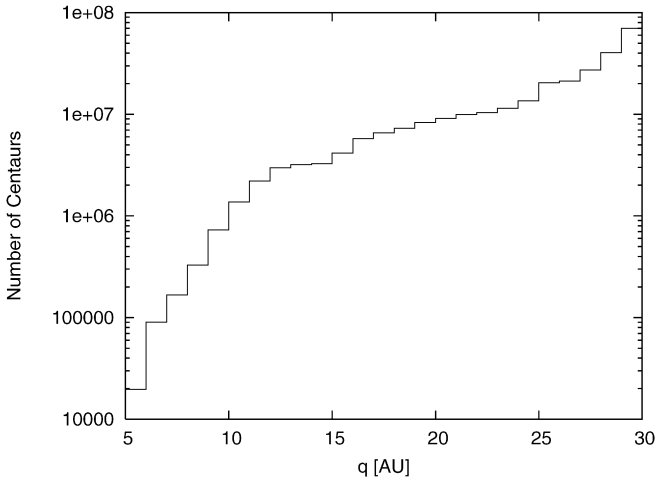


Fig. 8. Number of Centaurs (with $R > 1$ km) in perihelion bins.

current rate of injection of Centaurs (with $R > 1$ km) from the SD of 3.9 SDO/year and a population of $2.8 \times 10^8$ Centaurs with a radius greater than 1 km. However, the estimation of the number of SDOs by Fernández et al. (2004) has an uncertainty of nearly one order of magnitude; the number of SDOs with $R > 1$ km could be between $1.1 \times 10^9$ and $7.8 \times 10^{10}$. So our estimation of the number of Centaurs with $R > 1$ km would be between $4.1 \times 10^7$ and $2.9 \times 10^9$ and the current rate of injection from the SD would be between 0.6 and 41 SDO/year. We will adopt in the following the most likely value of $2.8 \times 10^8$ Centaurs with $R > 1$ km although one should bear in mind the uncertainty of nearly one order of magnitude of this estimation.

Levison and Duncan (1997) obtained a number of ecliptic comets with $H_T < 9$ ($R > \sim 1$ km) as $1.2 \times 10^7$. So, we can compare this estimation with our estimation of $N_C$ ($R > 1$ km) $= 2.8 \times 10^8$. As we see, the contribution to Centaurs from objects in the simulation of Levison and Duncan (1997) is one order of magnitude lower than our estimation of Centaurs, even the lower limit of our number of Centaurs is $\sim$3 times greater. We think this difference is due to the fact that Levison and Duncan (1997) integrated objects in low eccentricity and low inclination orbits occupying only a narrow fringe in semimajor axes. This is only a portion of the TN region and, on another hand, they are in more stable orbits than the SDOs' ones.

### 4.1. The distribution of Centaur perihelia

We have computed the normalized time-weighted perihelion distribution for the Centaurs in our simulation. Then, by multiplying this distribution by the total number of Centaurs (with $R > 1$ km) previously obtained, we plot in Fig. 8 the number of Centaurs (with $R > 1$ km) in perihelion bins. We can see an exponential growth in the number of Centaurs with perihelion.

## 5. Dynamical evolution in the Centaur zone

As we have already mentioned, the mean dynamical lifetime of a particle as a Centaur object is large and the question is, why? In order to answer this question we analyzed the behavior of the particles from our integration of SDOs in the Centaur zone. The objects that have the largest lifetimes show, in general terms, four types of dynamical characteristics, that keep their perihelion distances inside Neptune's orbit. These behaviors are simple or combined with each other.

The first type is characterized by the conservation of the perihelion distance for most of the particle lifetime as a Centaur, in a range of values between that of Saturn and Neptune's orbit. This is accompanied by the conservation or the very slow variation of the perihelion longitude, eccentricities greater than 0.8, and large semimajor axes (in general >100 AU). The characteristics of this evolution make the orbit go into a "pseudo-stable" state during which the encounters with planets are avoided or very weak, causing a very slow variation of the orbit orientation.

This kind of behavior is shown in Fig. 9. This figure shows the evolution of a synthetic object of the SDO 2000 SS331. This particle enters the planetary zone after an encounter with Neptune, and encounters with Uranus and Saturn. Then it keeps its perihelion distance between $\sim$15 and $\sim$20 AU having occasional encounters with Uranus. The eccentricity keeps greater than $\sim$0.7 and we can see a very slow variation of the longitude of perihelion in this period. This situation is maintained for $\sim 1.2 \times 10^8$ years till finally going to an hyperbolic ejection end state.

The second type of objects are those that show "resonance hopping" (this is a phenomenon in which objects move quickly from one resonance, in this case with Neptune, to another) combined with a behavior similar to the first one but with less constant eccentricity values and constant perihelion distances for shorter intervals of time. The semimajor axes, are in general, greater than 30 AU (although there are incursions to lower values) and less than 150 AU. The resonance hopping makes the object's perihelion stay in the giant planet zone going from one resonance to another, staying in each one for a period of time that goes from $10^5$ to $10^8$ years. Similar results were reported by Tiscareno and Malhotra (2003). This type of objects have also transfers between mean motion resonances and Kozai

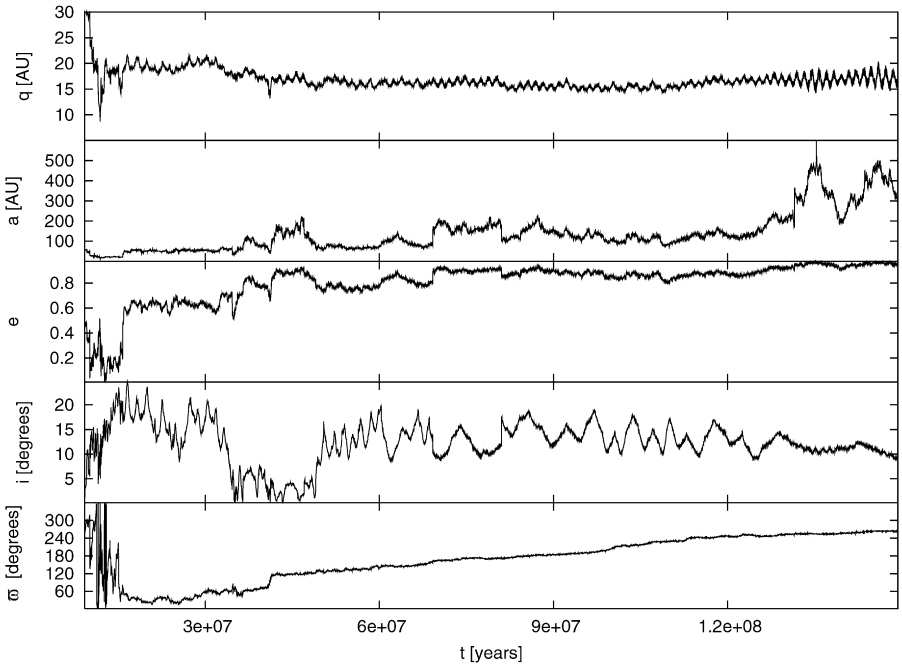


Fig. 9. Dynamical evolution of a synthetic SDO of the SDO 2000 SS331, with initial orbital elements: $a = 63.683$ AU, $e = 0.521$, $i = 5.35°$ and $q = 30.481$ AU. This object exemplifies the behavior of particles of the first type.

resonances. A Kozai resonance occurs when the argument of pericentre, $w$, librates about a constant value. For low inclinations it is possible for $w$ to librate about $w = 0°$ and $w = 180°$, and for large inclinations about $w = 90°$ and $w = 270°$. The semimajor axis of the object remains constant but the eccentricity and the inclination of the orbit are coupled in such a way that $e$ is a maximum when $i$ is a minimum, and vice versa. This transfer mechanism is shown in Fig. 10 with the evolution of a synthetic object of the SDO 1999 RZ215 (91554). This object enters the Centaur zone and then drops its $e$ and its $a$, and consequently, its $q$ go into the planetary zone, being finally ejected. In this route the object goes through mean motion resonances and also Kozai resonances where the argument of perihelion $w$ librates around $\sim 180°$.

We have lots of resonances populated, so we frequently have plutinos, and Neptune Trojans, for long periods of time. As an example, a synthetic object of the SDO 2000 QM251 remains in a 2:3 mean motion resonance with Neptune (i.e. a plutino), with an eccentricity that keeps in $\sim 0.35$ and an inclination of $\sim 14°$ for $6 \times 10^8$ years until it is quickly injected to the zone interior to Jupiter's orbit.

Resonance capture is a frequent state in the evolution of SDOs (Fernández et al., 2004), so it is not uncommon to have this behavior in the evolution of our particles.

In these two first types, the objects have casual encounters with Neptune and Uranus, sometimes also with Saturn, but they are not strong enough to drastically change their orbit. Only when the encounters with the planets begin to be more frequent, the object is unstable and goes to its final stage quickly; it is ejected to the Oort cloud or injected to the zone with $r < 5.2$.

In the third type of objects, we group those that have the behaviors of the first and second types, but they have perihelion distances near Neptune. So, the objects are continuously entering and leaving the Centaur zone. They could have a casual encounter with Uranus, but their dynamics are governed by Neptune.

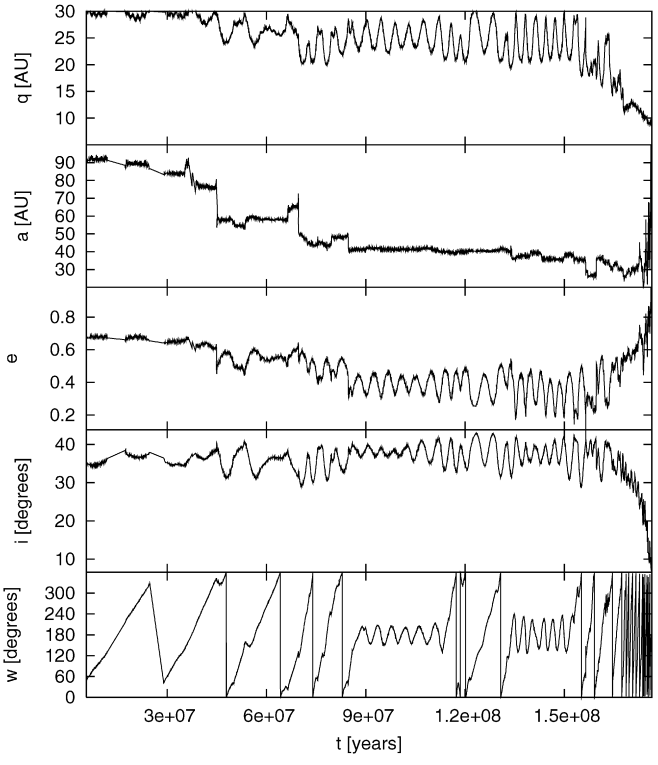


Fig. 10. Dynamical evolution of a synthetic SDO of the SDO 1999 RZ215 (91554) with initial orbital elements: $a = 100.99$ AU, $e = 0.692$, $i = 36.65°$ and $q = 31.1$ AU. We can see transfers between mean motion resonances and also Kozai resonances.

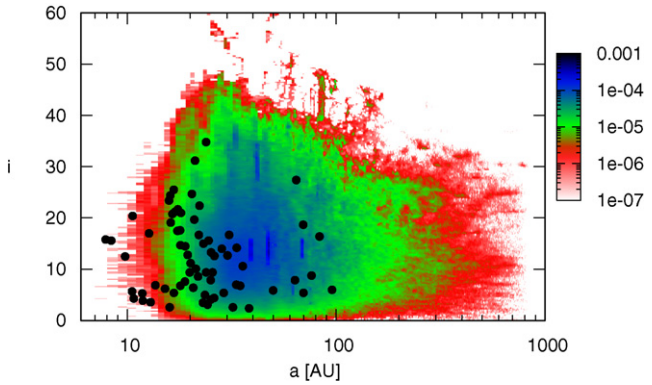


Fig. 11. Time-weighted distribution of the Centaurs obtained in the simulation in the semimajor axis ($a$) vs inclination ($i$) space. The circles are the observed Centaurs.

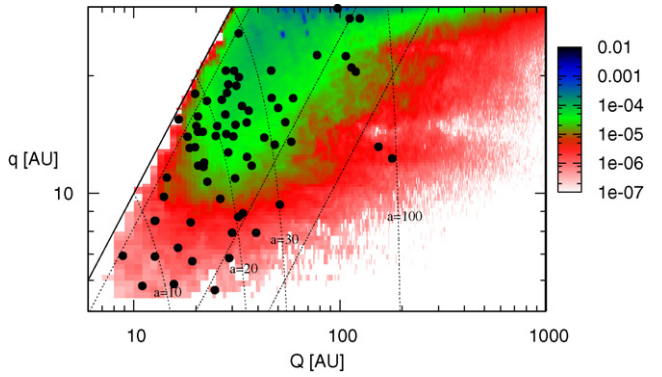


Fig. 12. Time-weighted distribution of the Centaurs obtained in the simulation in the perihelion ($q$) vs aphelion ($Q$) space. The circles are the observed Centaurs. The solid diagonal line corresponds to orbits of zero eccentricity and the dotted diagonal lines correspond to orbits with constant eccentricity of values 0.1, 0.6 and 0.8 from left to right. The curved dotted lines represent orbits with constant semimajor axis $a$, as is pointed to in the plot.

The last type of objects are those that enter a mean motion resonance or Kozai resonance for almost all their lifetime as a Centaur.

Finally, there are particles that exhibit a combination of the four types mentioned above, and also a "hand off" from the gravitational control of one planet to another.

When this hand off sends the particle near Jupiter, having close encounters with this planet, the object is either quickly ejected or injected to the inner Solar System. In all types, a long time and/or short time correlation is observed between the eccentricity and the inclination, which corresponds to the Tisserand parameter conservation. So, the general dynamics of these objects can be represented by the Restricted Three Body Problem.

In general, the types of behavior described above prevent strong close encounters with the planets, making the evolution in the giant planetary zone be a long term evolution (in particular between Saturn and Neptune).

The particles that have shorter lifetimes (say less than 1 Myr) carry out short incursions to the Centaur zone, having perihelion distances of no less than 28 AU, except for a few of them that cross the giant planetary zone to the zone interior to Jupiter's orbit.

## 6. Our model and the intrinsic Centaur population

### 6.1. Distribution of orbital elements

In order to study how the Centaur zone is populated, we plotted, in Figs. 11 and 12, the distribution of residence times (see Di Sisto et al., 2005) or the time-weighted distribution of Centaurs obtained in the simulation in the orbital element space. These plots represent the distribution of Centaurs in our model, assuming time-invariability. The observed Centaurs are also plotted. They are found in the zone also occupied by our sample. However, most of the observed Centaurs have perihelion distances of less than ∼20 AU and low semimajor axes. So, there is a zone of perihelion distances between 20 and 30 AU that, according to our model, must be densely populated, but we have observed only occasional objects there. It is also evident from Fig. 12 that when an object reaches perihelion distances of less than that of Saturn, the diffusion times are very short in contrast to the zone out of this planet. In Fig. 11, the instability of the region of low $a$ is also seen. It is also an unstable region at large $a$, this is artificial and a product of our cut in the simulation due to the non-validity of our model for large distances. Our model predicts a denser zone of semimajor axis between ∼20 and ∼80 AU, and inclinations between ∼5° and ∼30° and we didn't have inclinations greater that 60°.

In order to test the agreement between our model population and the observed population, we simulated an observationally biased survey of our model population. We followed the method adopted by Tiscareno and Malhotra (2003) with some small changes. We randomly assigned to the particles of our sample an absolute magnitude $H$ from the distribution law $N(< H) \sim 10^{aH}$. We adopted $a = 0.54$ from Larsen et al. (2001). From the heliocentric and geocentric distance of the object, we calculated the apparent magnitude $V$ (Bowell et al., 1989). We adopted a slope parameter $G$ of 0.15 for all Centaurs in our sample. $G$ is an indication of the gradient of the phase curve (reduced magnitude against phase angle). Then, following Tiscareno and Malhotra (2003), we extracted for the survey those objects with $V < 24$ and instantaneous ecliptic latitude $|\beta| < 5°$. We distributed the absolute magnitudes in the range $5 < H < 16.2$. The observed Centaurs have $H$ between 6 and 14.3, but we extended this range in our model to $H = 16.2$ [$R \sim 1.3$ km assuming an albedo of ∼0.09 (Brown and Trujillo, 2003)]. This value of $H$ corresponds of an object that have $V = 24$ at a distance from the Sun of 5.5 AU, that is, the nearest faintest observable Centaur. With this range of absolute magnitudes we are supposing that the magnitude distribution index (or the corresponding size distribution index) is the same up to kilometer sized objects.

Fig. 13 shows the normalized cumulative distribution of orbital elements of our Centaur survey and the observed Centaur population. In general, there is a good match between the two curves, though there are some differences. There is a notable lack of observed Centaurs in the range $30 < a < 50$ AU with respect to our survey. This is just the zone of low eccentricity classical KBO. So, this difference could be due to an erroneous

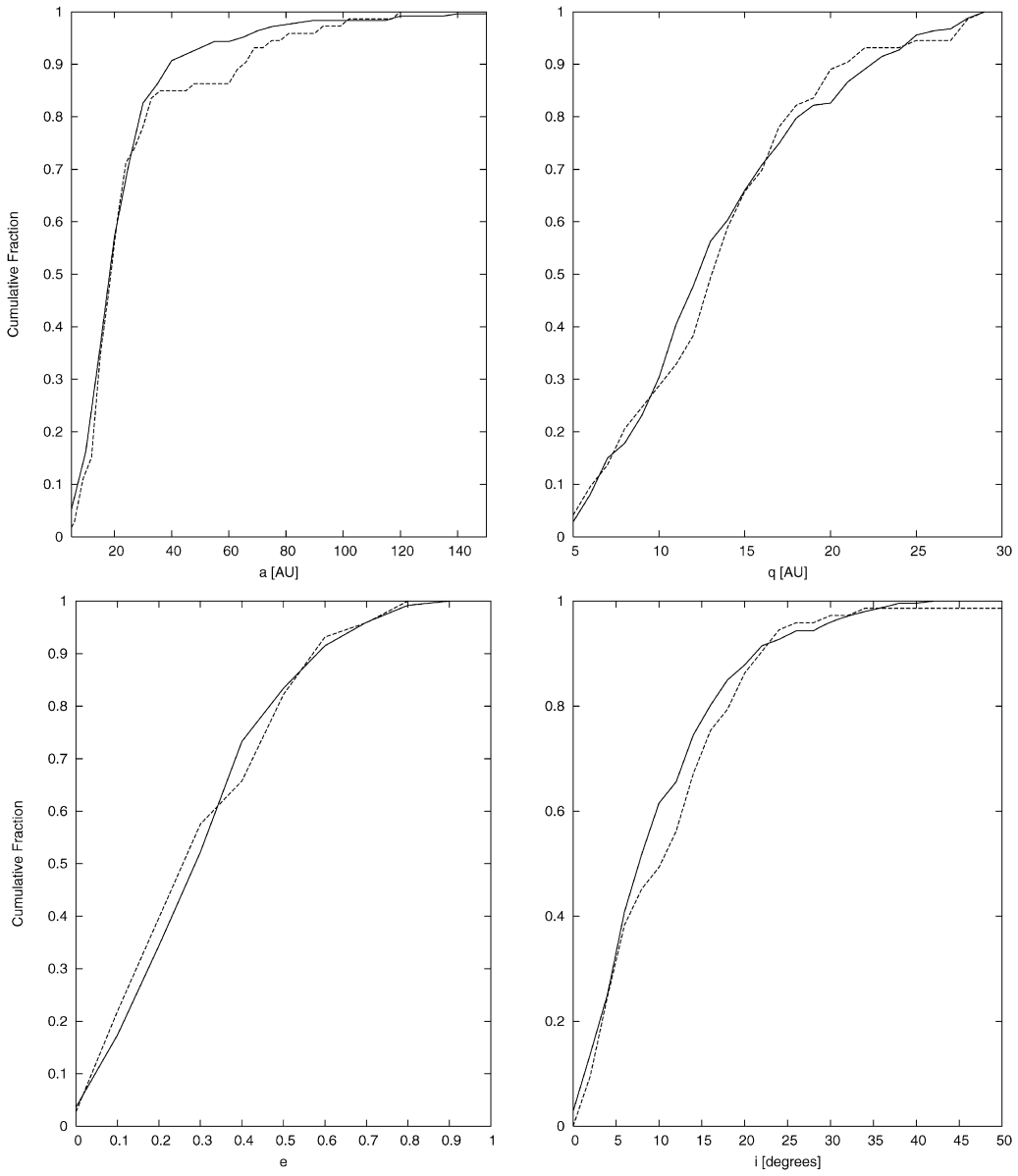


Fig. 13. Distribution of orbital elements of the observational survey generated with the Centaurs obtained in our simulation (solid line) and distribution of the observed Centaurs (dashed line).

eccentricity determination, making some objects that must be SDOs be cataloged as CKBOs. The correspondence in the perihelion distribution is quite similar. We can see that the observed Centaurs are a little biased to lower eccentricities. There is also a lack of observed inclinations between 5° and 10°, this could be due to the limitations of the inclination distribution model used for the source particles in the SD.

So, in view of the similarities shown in Fig. 13, it seems quite probable that our model of distribution of Centaurs could represent well the intrinsic orbital parameters distribution of the Centaur population. However, there are other likely sources for Centaurs that, though secondary sources, could affect the parameters involved in the survey previously revealed. But due to their supposed minor contribution, they would not modify the essence of the orbital parameter distribution obtained in our simulation.

### 6.2. Distance distribution

In Fig. 14 we plot the time-weighted distance distribution of the Centaurs in our simulation. The curve is normalized. This distribution is well fitted by a power law of the form $\mathrm{d}N/\mathrm{d}r \propto r^a$ where $\mathrm{d}N/\mathrm{d}r$ where $a \sim -1.49$ for $r > 30$ AU, a value a little greater than the one found in Levison and Duncan (1997) ($a = -1.8$) and nearly equal than that obtained by Tiscareno and Malhotra (2003) ($a = -1.5$). For $r < 30$ AU, we find $a \sim 4$. Those fits are also shown in the figure.

### 6.3. The big Centaurs

It is interesting to know how many large Centaurs there would be and how many would be observable. So, with the absolute magnitude distribution law for Centaurs that we have

considered, $N(<H) \sim 10^{0.54H}$, and taking into account the total number of Centaurs with $R > 1$ km previously obtained, it is possible to calculate the number of Centaurs greater than a given radius. In this calculation, we have to take into account the relation between radius and absolute magnitude, and select an albedo. Then, according to our model, the number of Centaurs greater than Chiron ($N$) would be between 360 and 650 for albedos between 0.05 and 0.09. But if we consider an apparent magnitude limit of $V = 24$, the observable objects must have a distance of less than 56 AU. Then, the observable number of Centaurs greater than Chiron ($H = 6.5$) will be $N_0 = F(<r)N$, where $F(<r)$ is the fraction of Centaurs with $r < 56$ AU. This fraction can be calculated from the normalized cumulative distance distribution of Centaurs of our model, we have $F(<56 \text{ AU}) = 0.37$. Then we obtained $N_0$ between 130 and 240.

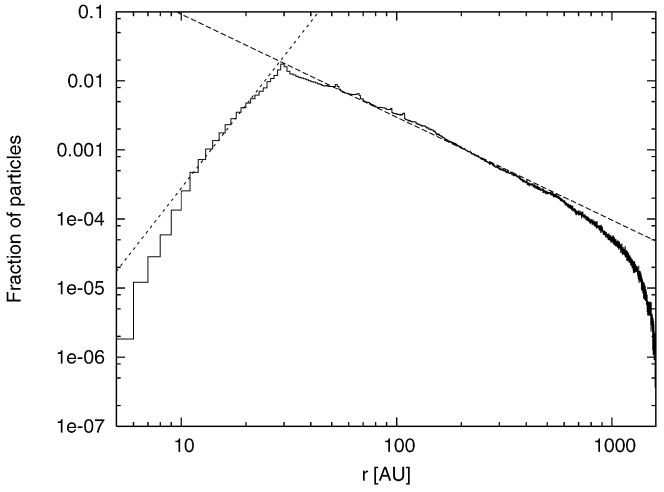


Fig. 14. Time-weighted distribution of radial distance of the Centaurs obtained in the simulation. The dotted lines are the power law fits discussed in Section 6.2.

We have at present, 4 Centaurs greater than Chiron and three of them have $r < 18$ AU. Our model predicts between 4 and 7 Centaurs greater than Chiron inside 18 AU. Then the total number of currently observed big Centaurs inside 18 AU could be almost complete.

### 6.4. Magnitude distribution

With the parameters defined in the simulated survey in the previous section, we calculated the apparent magnitudes ($V$) for all the Centaurs in our simulation. As mentioned in Section 6 we distributed the absolute magnitudes of our sample of Centaurs in the range $5 < H < 16.2$, where $H = 16.2$ ($R \sim 1.3$ ) corresponds to the nearest faintest observable Centaur. Then to compare, at first, the apparent magnitude distribution of Centaurs in our model with the apparent magnitude distribution of observed Centaurs we proceed as follows: we calculated the normalize distribution of our model, and restrict our sample to those with $|\beta| < 5°$. We multiply this distribution by the number of Centaurs greater than 1.3 km which is $N_C(H < 16.2) = 1.3 \times 10^8$ (from the magnitude distribution given in Section 6.1 and the total number of Centaurs with $R > 1$ km previously obtained). In Fig. 15a we show the observed magnitude distribution and the magnitude distribution of Centaurs from our model with $|\beta| < 5°$ and $R > 1.3$ km. As we can see there would be a great difference between our model and the observed population.

But the real observed Centaurs discovered up to now have $H$ between 6 and 14.3, (or radius between ∼1 and ∼3 km) so there are some Centaurs with $H$ between 14.3 and 16.2 that could have been discovered but up to now, they were not. So for really testing if our model match the observations we have to restrict our sample of Centaurs both to those with $|\beta| < 5°$ and to those of $H < 14.3$. That are the conditions for the real discovered Centaurs. So, we must multiply the normalized distribution restricted to $|\beta| < 5°$ by the number of Centaurs with $H < 14.3$

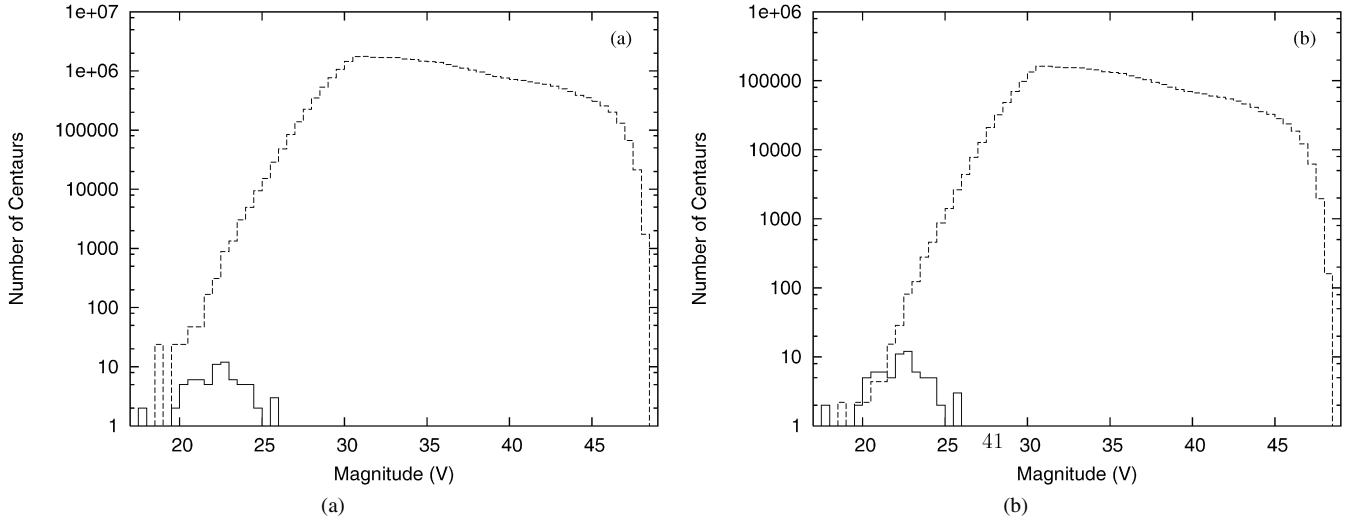


Fig. 15. (a) Number observed Centaurs versus the apparent magnitude (solid line) and magnitude distribution of Centaurs from our model with $|\beta| < 5°$ and $H < 14.3$ (dashed line) with which the observed distribution must be compared. (b) Apparent magnitude distribution of Centaurs with $R > 1$ km (dashed line) and of observed Centaurs (solid line).

($N_C(H < 14.3) = 1.2 \times 10^7$). This comparison of the apparent magnitude distributions is plotted in Fig. 15b.

As we can see, the magnitude distribution of Centaurs from our model with $|\beta| < 5°$ and $H < 14.3$ nearly agrees with the magnitude distribution of observed Centaurs for $V < \sim 22$. Although this value of $V$ is not the limit of the present observability, it is very near, and objects with greater values of $V$ are difficult to detect. That's probably why there may not be an agreement on these values. So, once again we can say that our model fits well with observations.

Besides, we can see, according to our model, that there must be lots of Centaurs with small radii (at least with $R$ between $\sim 1$ and $\sim 3$ km), that would have apparent magnitudes and ecliptic latitudes in the ranges of observability, but they have not been discovered so far. To be found, such objects must be near the inner edge of the Centaur region. Centaurs to date have been discovered in a very unsystematic way by Kuiper belt and NEO surveys. Kuiper belt surveys are targeted to objects that move more slowly than Centaurs, and NEO surveys are targeted to fast-moving objects, so Centaurs fall "in the cracks" between. Kuiper belt surveys often impose a limit on the rate of motion in order to avoid being burdened by lots of asteroids, and the efficiency of the NEO surveys for Centaurs is very low. That's why our model do not agree with the observations of very small Centaurs.

If our model represents the intrinsic population, one can see from Fig. 15 that the vast majority of Centaurs have apparent magnitudes outside the current limit of observability.

## 7. Conclusions

We have evolved objects from the SD and studied their end states. 25.8% of the particles survive the total integration time, 51.9% are ejected from the Solar System, and 21.8% enter the zone of $r < 5.2$ AU. The relation $N_e/N_s$ (where $N_s$ is the number of survivor particles and $N_e$ the number of ejected particles) is inverted at $q = 35$ AU and $a > 50$ AU. The SD zone of $q < 35$ AU and $40 < a < 50$ AU is the most efficient in reaching the JFC end state. The zone of $q < 35$ AU is the most efficient in injecting Centaurs. 75.5% of SDOs enter the Centaur zone, having there a mean lifetime ($l_C$) of 72 Myr. 30% of this Centaurs reach the zone of $r < 5.2$ AU.

The mean lifetime is dependent on the initial inclination of particles, those with $i_i < 16°$ have $l_C = 42$ Myr. This is comparable with the mean lifetime of ecliptic comets obtained by Levison and Duncan (1997) of 45 Myr. The high inclinations in objects of the SD make Centaurs long lived objects.

The mean lifetime of Centaurs is strongly dependent on their perihelion distances. In the zone of low perihelion distances we have mean lifetimes of the order of Myr, e.g. 10 Myr for Centaurs with $q < 17$ AU and also in a zone $5.2 < a < 30$ is 7.6 Myr; those numbers are comparable with previous works.

SDOs are probably the main source for Centaurs providing a current number of $\sim 2.8 \times 10^8$ Centaurs with $R > 1$ km. A secondary source are unstable trans-neptunian objects in low eccentricity orbits according to the estimation of Levison and Duncan (1997) of $1.2 \times 10^7$.

We described some mechanisms that kept perihelion distances of particles inside Neptune orbit for long periods of time. Those are: the conservation of $q$ in narrow ranges between Saturn and Neptune, resonance hopping or capture in a mean motion or Kozai resonances for long intervals of time that could reach the Gyr.

We also generated a survey with our sample of Centaurs to test whether the distribution of orbital elements obtained in our simulation could represent the intrinsic distribution. With the parameters described above, our survey match well with the observed sample of Centaurs, so the distribution of Centaurs described in Figs. 11 and 12 could be a model for the intrinsic distribution. However, the indices of the absolute magnitude distribution of Centaurs may change with the improvement of the observations and with the contribution of other sources to the Centaur population as escaped plutinos.

The distribution of distances is well fitted by a power law of the form $\Sigma \propto r^a$ where $a \sim -1.49$ for $r > 30$ AU, and $a \sim 4$ for $r < 30$ AU.

The magnitude distribution shows that there must be lots of small Centaurs, with a radius at least between 1 and 3 km, that would have apparent magnitudes and ecliptic latitudes in the ranges of observability that have not been discovered yet. This fact is related with inefficiency of present minor objects surveys in finding Centaurs. Besides, there must still be more Centaurs in the range of apparent magnitudes outside the current limit of observability.

## Acknowledgments

We are grateful to José L. Ortiz for his suggestions and comments. Special thanks to Luke Dones for his comments on the distance and magnitude distribution of Centaurs. We also acknowledge an anonymous referee and M.S. Tiscareno for their criticism and suggestions that helped us to improve the manuscript.

We acknowledge the financial support given by IALP, CONICET and of Agencia de Promoción Científica, through the Grant PICT 03-11044.

## References

Bowell, E., Hapke, B., Domingue, D., Lumme, K., Peltoniemi, J., Harris, A.W., 1989. Application of photometric models to asteroids. In: Binzel, R.P., Gehrels, T., Matthews, M.S. (Eds.), Asteroids, vol. II. Univ. of Arizona Press, Tucson, pp. 524–556.

Brown, M.E., 2001. The inclination distribution of the Kuiper Belt. Astron. J. 121, 2804–2814.

Brown, M.E., Trujillo, C.A., 2003. Direct measurements of the size of the large Kuiper Belt object (50000) Quaoar. Astron. J. 127, 2413–2417.

Chiang, E., Lithwick, Y., Murray-Clay, R., Buie, M., Grundy, W., Holman, M., 2006. A brief history of trans-neptunian space. In: Reipurth, B., Jewitt, D., Keil, K. (Eds.), Protostars and Planets V. Univ. of Arizona Press, Tucson, in press.

Di Sisto, R.P., Brunini, A., Dirani, L.D., Orellana, R.B., 2005. Hilda asteroids among Jupiter family comets. Icarus 174, 81–89.

Duncan, M., Levison, H., 1997. Scattered comet disk and the origin of Jupiter family comets. Science 276, 1670–1672.

Duncan, M., Quinn, T., Tremaine, S., 1988. The origin of short-period comets. Astrophys. J. 328, 69–73.

Elliot, J.L., Kern, S.D., Clancy, K.B., Gulbis, A.A.S., Millis, R.L., Buie, M.W., Wasserman, L.H., Chiang, E.I., Jordan, A.B., Trilling, D.E., Meech, K.J., 2005. The deep ecliptic survey: A search for Kuiper Belt objects and Centaurs II. Dynamical classification, the Kuiper Belt plane, and the core population. Astron. J. 129, 1117–1162.

Emel'yanenko, V.V., Asher, D.J., Bailey, M.E., 2005. Centaurs from the Oort cloud and the origin of Jupiter family comets. Mon. Not. R. Astron. Soc. 361, 1345–1351.

Fernández, J.A., 1980. On the existence of a comet belt beyond Neptune. Mon. Not. R. Astron. Soc. 192, 481–491.

Fernández, J.A., Gallardo, T., Brunini, A., 2002. Are there many inactive Jupiter family comets among the near-Earth population? Icarus 159, 358–368.

Fernández, J.A., Gallardo, T., Brunini, A., 2004. The scattered disk population as a source of Oort cloud comets: Evaluation of its current and past role in populating the Oort cloud. Icarus 172, 372–381.

Gladman, B., Holman, M., Grav, T., Kavelaars, J., Nicholson, P., Aksnes, K., Petit, J.-M., 2002. Evidence for an extended scattered disk. Icarus 157, 269–279.

Gomes, R.S., 2002. The origin of the Kuiper Belt high-inclination population. Icarus 161, 404–418.

Horner, J., Evans, N.W., Bailey, M.E., 2004a. Simulations of the population of Centaurs. I. The bulk statistics. Mon. Not. R. Astron. Soc. 354, 798–810.

Horner, J., Evans, N.W., Bailey, M.E., 2004b. Simulations of the population of Centaurs. II. Individual objects. Mon. Not. R. Astron. Soc. 355, 321–329.

Larsen, J.A., Gleason, A.E., Danzi, N.M., Descour, A.S., McMillan, R.S., Gehrels, T., Jedicke, R., Montani, J.L., Scotti, J.V., 2001. The spacewatch wide-area survey for bright Centaurs and trans-neptunian objects. Astron. J. 121, 562–579.

Levison, H., Duncan, M., 1997. From the Kuiper Belt to Jupiter family comets: The spatial distribution of ecliptic comets. Icarus 127, 13–32.

Morbidelli, A., Emel'yanenko, V., Levison, H.F., 2003. Origin and orbital distribution of the trans-neptunian scattered disk. Mon. Not. R. Astron. Soc. 335, 935–940.

Tiscareno, S.M., Malhotra, R., 2003. The dynamics of known Centaurs. Astron. J. 126, 3122–3131.